

# Spindle Microtubule Differentiation and Deployment during Micronuclear Mitosis in *Paramecium*

JOHN B. TUCKER, SALLY A. MATHEWS, KAY A. K. HENDRY, JOHN B. MACKIE, and DAVID L. J. ROCHE

Department of Zoology and Marine Biology, University of St. Andrews, St. Andrews, Fife KY16 9TS, United Kingdom

**ABSTRACT** Spindles underwent a 12-fold elongation before anaphase B was completed during the closed mitoses of micronuclei in *Paramecium tetraurelia*. Two main classes of spindle microtubules have been identified. A peripheral sheath of microtubules with diameters of 27–32 nm was found to be associated with the nuclear envelope and confined to the midportion of each spindle. Most of the other microtubules had diameters of ~24 nm and were present along the entire lengths of spindles. Nearly all of the 24-nm microtubules were eliminated from spindle midportions (largely because of microtubule disassembly) at a relatively early stage of spindle elongation. Disassembly of some of these microtubules also occurred at the ends of spindles. About 60% of the total microtubule content of spindles was lost at this stage. Most, perhaps all, peripheral sheath microtubules remained intact. Many of them detached from the nuclear envelope and regrouped to form a compact microtubule bundle in the spindle midportion. There was little, if any, further polymerization of 24-nm microtubules after the disassembly phase. Polymerization of microtubules with diameters of 27–32 nm continued as spindle elongation progressed. Most microtubules in the midportions of well-elongated spindles were constructed from 14–16 protofilaments. A few 24-nm microtubules with 13 protofilaments were also present. The implications of these findings for spatial control of microtubule assembly, disassembly, positioning, and membrane association, that apparently discriminate between microtubules with different protofilament numbers have been explored. The possibility that microtubule sliding occurs during spindle elongation has also been considered.

Until early anaphase the organization of a mitotic spindle in a dividing micronucleus of *Paramecium tetraurelia* is not markedly different from that of mitotic spindles in general (11, 23). This is also the case for mitotic spindles in other members of the *Paramecium aurelia* complex of sibling species (30) that have been examined (16, 17, 32). However, anaphase B (chromatid separation promoted by an increase in pole-to-pole distance) (13) is extremely pronounced. For example, a nucleus elongates from ~7  $\mu\text{m}$  (at metaphase) to ~90  $\mu\text{m}$  before its division is completed in *P. tetraurelia*. A bundle of microtubules extends between the two sets of separating sister chromatids as this occurs. These bundles may be homologous with the interzonal microtubule arrays present during late anaphase and telophase in the spindles of other organisms (25). They have been usefully referred to as separation spindles by previous investigators (34).

Certain separation spindles are of special interest in the context of control of microtubule differentiation and deployment for two main reasons. (a) Two classes of microtubules have been found at some stages in the elongation of separation spindles, and (b) there is a marked change in spindle microtubule organization at a relatively early stage of separation spindle elongation. For example, one class of microtubules forms a peripheral sheath around each spindle in *Tetrahymena thermophila* (6, 21, 22), *Paramecium bursaria* (24), and *Nyctotherus ovalis* (7, 9, 10). Each sheath is a single layer of microtubules that is closely associated with the inner surface of the nuclear envelope. This is one feature that distinguishes peripheral sheath microtubules from the other microtubules in a spindle. In *Nyctotherus*, sheath microtubules are more stable than the other microtubules during early anaphase. Sheath-like arrays of microtubules also occur in the elongating

meiotic micronuclei of *Tetrahymena thermophila* (6, 37), *Paramecium tetraurelia* (15), and *Ephelota gemmipara* (12). A peripheral sheath has been identified in this study of separation spindles in *P. tetraurelia*. In addition, most metaphase spindle microtubules have diameters of 24 nm in this organism, but most microtubules in well-elongated separation spindles have diameters of 27–32 nm and are composed of more than 13 protofilaments (5, 11, 35). Similar features have been reported for micronuclear mitosis in *Nyctotherus* (8, 10, 11). Microtubules with 13 protofilaments predominate during the early stages of mitosis. These microtubules disassemble when exposed to low temperatures and antimetabolic drugs. However, most of the microtubules in well-elongated separation spindles are cold and drug stable and are composed of more than 13 protofilaments. Changes in the pattern of spindle birefringence in *Spirostomum teres* also indicate that an abrupt and substantial change in spindle microtubule organization occurs at a relatively early stage of separation spindle elongation (14).

This investigation has mainly been concerned with establishing whether there is evidence for selective spatial control of the positioning, assembly, disassembly, and membrane-association of microtubules with different numbers of protofilaments. It also examines the question of how the different classes of microtubules are exploited during spindle elongation.

## MATERIALS AND METHODS

*Paramecium tetraurelia* (stock d4-2) was cultured (36), prepared for routine transmission electron microscopy (34), and in some cases fixed in the presence of tannic acid for subsequent examination of microtubule protofilaments (11), using procedures described previously. Measurements of microtubule diameters were made on micrographs taken at a microscope magnification of 29,000. Microscope magnification was determined by measuring lattice spacings of negatively stained catalase crystals (38).

Spindle lengths were assessed by recording the number of thick (1  $\mu\text{m}$ ) and thin sections (average thickness 86 nm) cut during the course of cross-sectioning from one end of a spindle to the other. Section thicknesses were assessed using procedures similar to those described elsewhere (22). Cross-sections of dividing spindles were obtained by cutting cross-sections of dividing organisms. During the later stages of spindle elongation both an organism's two micronuclei and their separation spindles were usually oriented parallel to an organism's longitudinal axis. These stages in spindle elongation were temporally correlated with stages in the constriction of the cleavage furrow that could be distinguished using a dissecting microscope after organisms had been fixed and flat-embedded. Cleavage had not started in organisms that contained nuclei and spindles at earlier stages of elongation. Such organisms exhibited a slight bulging of the putative furrow region. This could be detected when living organisms were examined using a dissecting microscope but was difficult to distinguish after fixation and embedding. Organisms with bulges were removed from cultures with a fine pipette and prepared individually for electron microscopy.

Such organisms contained nuclei that ranged from metaphase to stages at which they had undertaken up to half of their elongation. Furthermore, these nuclei were rarely oriented parallel to the longitudinal axes of organisms. As a consequence, sequences of sections that permitted accurate assessments of microtubule diameters and microtubule number/spindle cross-section were only obtained for three spindles at relatively early stages of spindle elongation. However, somewhat oblique sections of several other early spindles provided enough information about spindle dimensions and microtubule positioning (sometimes after section tilting in a goniometer specimen stage) to establish that the three well-oriented spindles were not atypical.

## RESULTS

### Micronuclear Elongation

Metaphase micronuclei were spheroidal in shape and slightly elongate with respect to their polar axes. Spindle microtubules were present along the entire lengths of nuclei. Thus, metaphase spindle length was the same as nuclear length ( $\sim 7 \mu\text{m}$ ) at this stage. Shortly after separation of sister chromatids had occurred, each elongating nucleus assumed a dumb-bell shape that persisted throughout the remaining stages of mitosis. The two sets of sister chromatids were located in the two lobe-shaped terminal knobs of each nucleus that were connected by the slender central portion of a nucleus (Fig. 1). This slender central portion elongated as anaphase B progressed, and most separation spindle microtubules were confined to this portion of a nucleus. The lengths of separation spindles referred to below represent the lengths of the slender central portion of each nucleus between its terminal knobs. Terminal knobs had lengths of  $\sim 4.5 \mu\text{m}$ , and this dimension did not change appreciably during separation spindle elongation. Hence, the length of a separation spindle was  $9 \mu\text{m}$  shorter than nuclear length throughout the main phase of nuclear elongation. Terminal knobs pinched off from the central spindle-containing portions of nuclei at a point when spindles had reached lengths of  $\sim 83 \mu\text{m}$ . This final stage of division was reached  $\sim 9$  min after metaphase at  $27^\circ\text{C}$  (36). Hence, spindles were elongating from 7 to  $\sim 80 \mu\text{m}$  at a mean rate of 8  $\mu\text{m}/\text{min}$ .

### Changes in Microtubule Content and Number during Spindle Elongation

Changes in the number of microtubule profiles/spindle cross-section at points along the lengths of spindles at four stages in spindle elongation are summarized in Fig. 2, *a-d*. Such data was obtained from serial cross-sections of one 21- $\mu\text{m}$ -long spindle (Fig. 2*a*), one 34- $\mu\text{m}$ -long spindle (Fig. 2*b*), one 45- $\mu\text{m}$ -long spindle (Fig. 2*c*), and three spindles with lengths in the range 62–69  $\mu\text{m}$ . A graph of the data for one

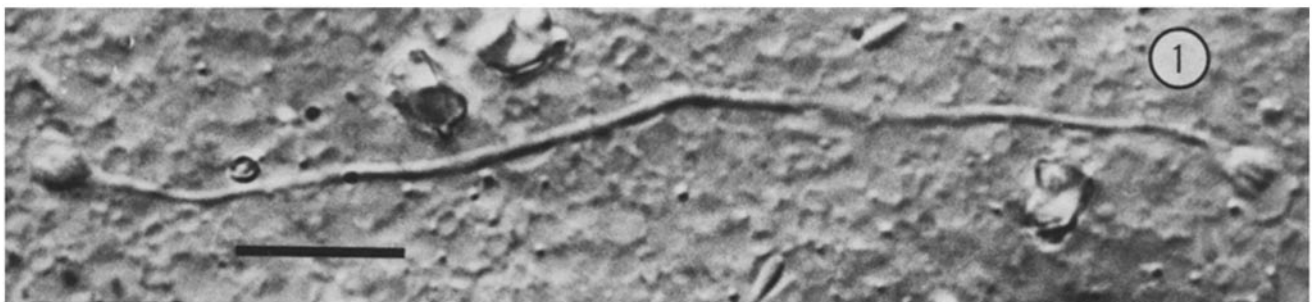


FIGURE 1 A dividing micronucleus showing its two terminal knobs and the intervening separation spindle-containing portion. Unfixed organism partially lysed in culture medium by compression between the microscope slide and coverslip. Differential interference contrast. Bar, 10  $\mu\text{m}$ .  $\times 2,200$ .

of the latter is shown in Fig. 2*d*; graphs for the other two were very similar. The number of microtubules/spindle cross-section was always greatest near spindle midpoints and decreased progressively on either side of this point as spindle extremities were approached.

Evidence for an abrupt change in spindle organization at a relatively early stage of spindle elongation was obtained from comparisons of the distributions of microtubule number/

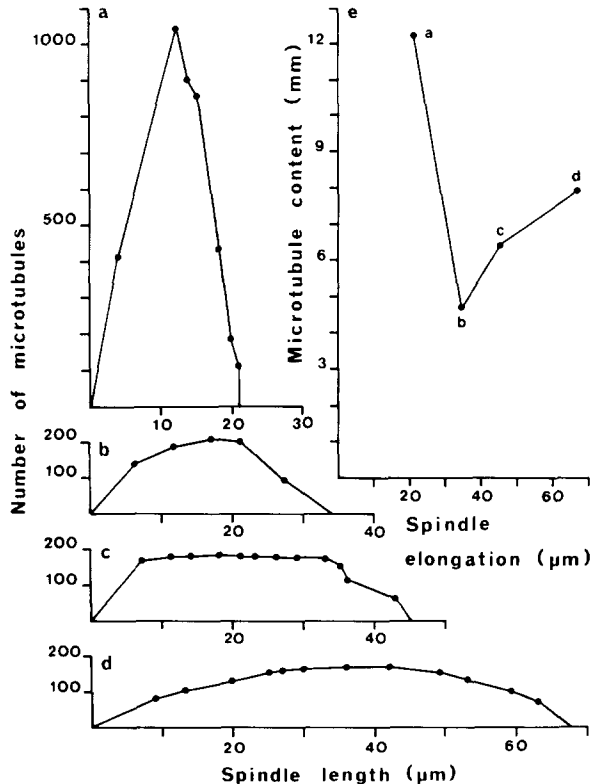


FIGURE 2 Graphs *a-d* show the number of microtubules/spindle cross-section at different distances from one end of each of four spindles (with lengths of 21, 34, 45, and 67 μm, respectively). The changes in microtubule content that occur as spindles elongate (based on spindles *a-d*) are shown in *e*.

spindle cross-section at different stages of spindle elongation (Fig. 2, *a-d*). More than 1,000 microtubules/cross-section were found near the middle of a 21-μm-long spindle (Fig. 2*a*), but the middle of a 34-μm-long spindle (Fig. 2*b*) possessed only 219 microtubules. After this markedly drop in number, microtubule number/spindle cross-section near the middles of spindles remained within a range of 169–228 microtubules for all spindles examined as spindles elongated from 34 to 72 μm (Fig. 2, *b-d*).

The data plotted in Fig. 2, *a-d* was used to estimate the total length of microtubules in individual spindles assuming that all of a spindle's microtubules were laid out end-to-end in a single linear array. This parameter is referred to as the microtubule content of a spindle (22). For example, a spindle with a length of 10 μm that includes exactly 100 microtubules at all points along its length has a microtubule content of 1,000 μm. Microtubule content has been assessed for each spindle represented in Fig. 2, *a-d* by calculating the area bounded by the plotted line and the abscissa. Microtubule content was 62% less in the 34-μm-long spindle than in the 21-μm-long spindle, but increased again by 37 and 69%, as spindles elongated to 45 and 67 μm, respectively (Fig. 2*e*).

Detailed tracking of individual microtubules to establish the positions of their ends and assess their lengths has not yet been undertaken. However, indications were obtained that microtubules have considerable lengths. For example, microtubule number/spindle cross-section in the midportions of well-elongated spindles remained constant for distances of up to 5 μm in some instances. Furthermore, this number decreased and never increased in sections cut progressively from a spindle middle toward the ends of a spindle. These findings are compatible with the possibility that most of the microtubules, near the middles of spindles with lengths of more than ~30 μm, span the middle of a spindle and terminate in a staggered fashion as they approach the ends of spindles.

### The 21-μm-long Spindle

A single layer of peripheral sheath microtubules was located around the main body of the midportion of this spindle. These microtubules were situated just inside the nuclear en-

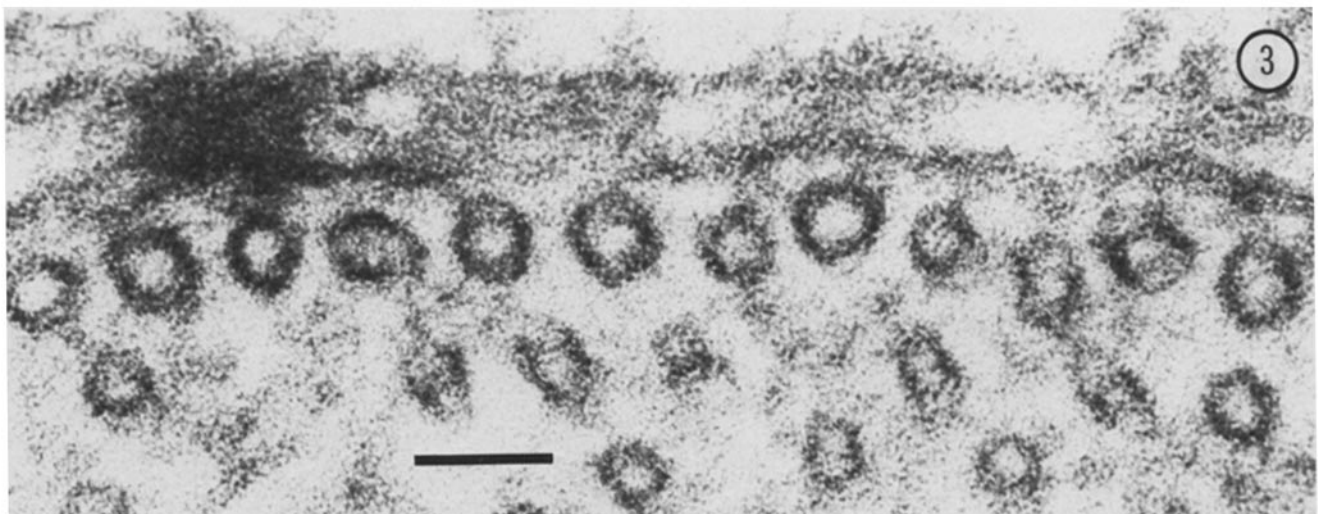


FIGURE 3 Cross-section through a portion of a 21-μm-long spindle cut 1.5 μm from the spindle midpoint. Most of the microtubules included in the single layer adjacent to the nuclear envelope have greater diameters than the other spindle microtubules. Bar, 50 nm. × 360,000.

velope and appeared to be bridged to it by fine strands of dense material at several points. Nearly all the sheath microtubules had diameters of 27–32 nm. This feature distinguished them from most of the remainder of the microtubules in the spindle that had diameters of ~24 nm (Fig. 3). For example, 816 of the 878 microtubules counted inside a sheath of 164 microtubules near the spindle midpoint (Fig. 4) had diameters of ~24 nm; the other 62 microtubules inside the sheath had diameters of 27–32 nm and were apparently randomly distributed among the 24-nm microtubules inside the sheath. Very few microtubules that had diameters of 27–32 nm, but which were not situated peripherally as part of the sheath, were found in sections cut more than 3  $\mu\text{m}$  from the spindle midpoint.

The relative shortness of this spindle, and the fact that a sheath was present which did not extend along the entire length of the spindle, was not appreciated until after sectioning of the spindle had progressed beyond its midpoint. Thin sections were not cut closer than 1.5  $\mu\text{m}$  to the spindle midpoint, or at a sufficiently close series of intervals to ascertain the exact length of the sheath. The sheath included 164, 139, and 129 microtubules at points situated 1.5  $\mu\text{m}$  (Fig. 4), 3  $\mu\text{m}$ , and 4.5  $\mu\text{m}$ , respectively, to one side of the spindle midpoint. The sheath was not present at any loci (Fig. 5) sectioned more than 6.5  $\mu\text{m}$  to one side of the midpoint and 7.5  $\mu\text{m}$  on the other. Assuming that the sheath is positioned symmetrically about the spindle midpoint, the above data indicate that the sheath was <13  $\mu\text{m}$  and >9  $\mu\text{m}$  in length,

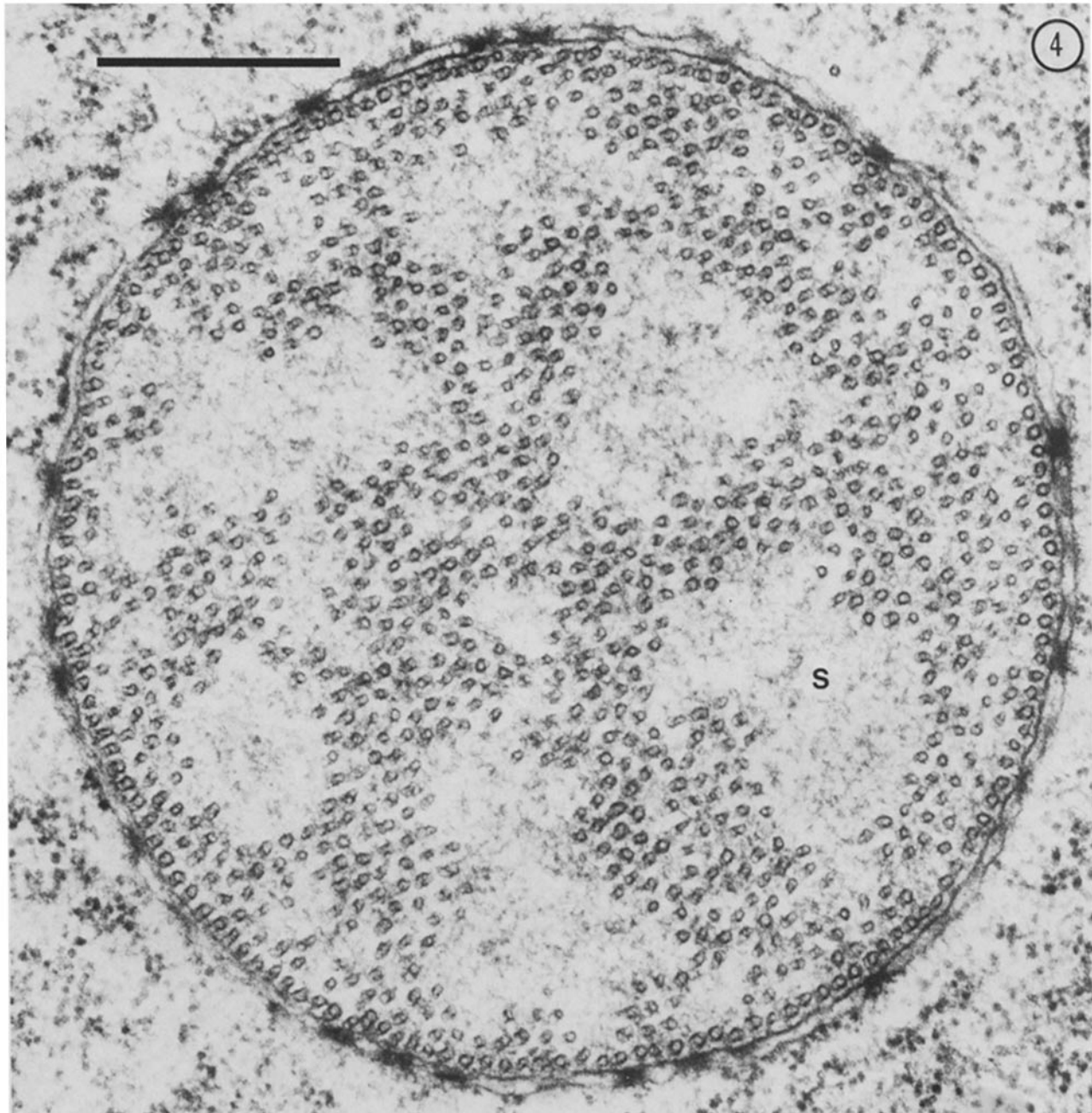
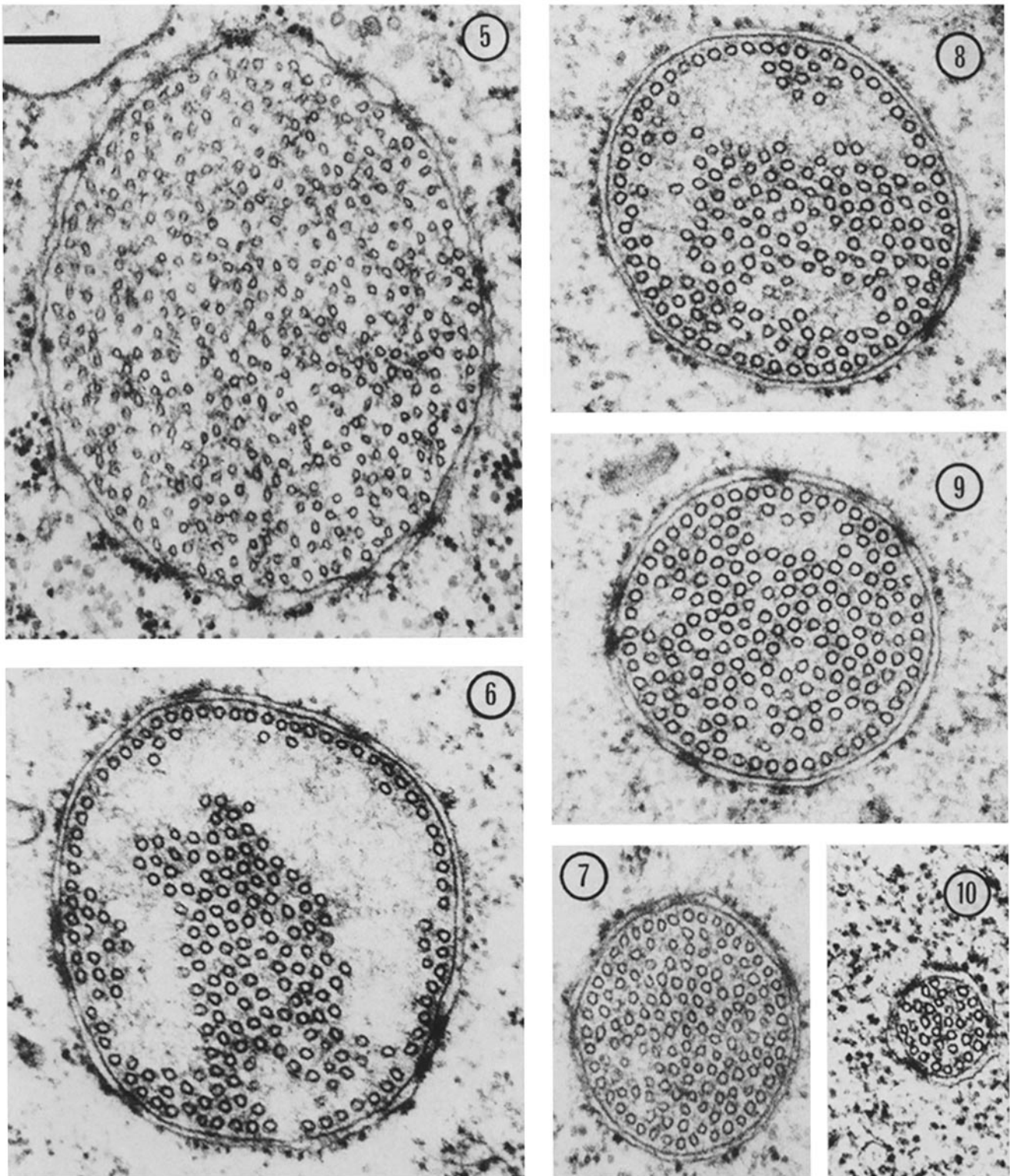


FIGURE 4 Cross-section of a 21- $\mu\text{m}$ -long spindle cut 1.5  $\mu\text{m}$  from the spindle midpoint. The peripheral microtubule sheath extends around the entire perimeter of the cross-sectional profile of the spindle. Spaces that are devoid of microtubules are occupied by an irregular meshwork of dense strands (S). Bar, 0.5  $\mu\text{m}$ .  $\times 75,000$ .



FIGURES 5-10 Cross-sections of separation spindles that are all presented at the same magnification ( $\times 75,000$ ). Bar,  $0.2 \mu\text{m}$ . (Fig. 5) Cross-section of a  $21\text{-}\mu\text{m}$ -long spindle cut  $6.5 \mu\text{m}$  from the spindle midpoint. A peripheral sheath cannot be distinguished (compare with the section of this spindle shown in Fig. 4). (Fig. 6) Cross-section at the midpoint of a  $34\text{-}\mu\text{m}$ -long spindle showing the peripheral sheath and the hollowed out appearance of spindle midportions at this stage. (Fig. 7) Cross-section of a  $34\text{-}\mu\text{m}$ -long spindle cut  $11 \mu\text{m}$  from the spindle midpoint. Most of the microtubules shown here have smaller diameters than most microtubules at the midpoint of this spindle which is shown in Fig. 6. (Fig. 8) Cross-section at the midpoint of a  $45\text{-}\mu\text{m}$ -long spindle. Microtubules are packed in a more compact array than they are at the midpoint of the  $34\text{-}\mu\text{m}$ -long spindle (compare Fig. 6). (Fig. 9) Cross-section at the midpoint of a  $65\text{-}\mu\text{m}$ -long spindle. (Fig. 10) Cross-section close to the end (within  $0.5 \mu\text{m}$  of the terminal knob) of a  $74\text{-}\mu\text{m}$ -long spindle. Microtubule diameters are smaller than those of most microtubules in the spindle midportions of well-elongated spindles (compare with Fig. 9).



and that the number of microtubules in the sheath decreased gradually from its midpoint toward its ends.

Microtubules were packed fairly evenly and closely alongside each other along much of the spindle, but along the portion surrounded by the sheath several large spaces devoid of microtubules occurred in the array (Fig. 4, 5). These spaces contained strands of dense material that seemed to form a loose meshwork.

### Spindles with Lengths of 34–45 $\mu\text{m}$

A 34- $\mu\text{m}$ -long spindle possessed 219 microtubules at its midpoint and nearly all of these had diameters of 27–32 nm. A single layer of microtubules arranged in a fashion similar to that of microtubules in the peripheral sheath in the 21- $\mu\text{m}$ -long spindle was apparent for distances of  $\sim 10 \mu\text{m}$  on either side of the spindle midpoint. Along this midportion of the spindle most of the remainder of the microtubules were bundled closely together. A substantial space or spaces devoid of microtubules was present for distances of  $\sim 4 \mu\text{m}$  to either side of the spindle midpoint so that the midportion of the spindle had a hollowed-out appearance (Fig. 6). A distinct sheath was lacking in the terminal portions of the spindle (Fig. 7). Microtubules with diameters of  $\sim 24 \text{ nm}$  formed an increasingly greater proportion of the spindle as spindle extremities were approached (compare Figs. 6 and 7). No microtubules with diameters detectably  $>24 \text{ nm}$  were found at points situated  $<7 \mu\text{m}$  from the ends of the spindle.

Microtubule deployment in a 45- $\mu\text{m}$ -long spindle was very similar to that in the 34- $\mu\text{m}$ -long spindle. Near the spindle midpoint spaces devoid of microtubules were present but were smaller than those in the 34- $\mu\text{m}$ -long spindle, so that in this region the spindle microtubule array was more compact in the longer spindle (compare Figs. 6 and 8).

### Well-elongated Spindles

Several spindles with lengths of 60–72  $\mu\text{m}$  were examined. They were all very similar in structure. They were not markedly different (lengths excepted) from the 45- $\mu\text{m}$ -long spindle described above apart from the finding that near their midpoints microtubules were grouped in a slightly more compact fashion than those in the 45- $\mu\text{m}$ -long spindle (compare Figs. 8 and 9). At spindle midpoints the numbers of microtubules ranged between 169 and 178. Along most of the lengths of the spindles most microtubules had diameters of 27–32 nm. Approximately 14% of the microtubules in spindle midportions had diameters of  $\sim 24 \text{ nm}$  (Fig. 11). However, this was not the case at spindle extremities. As in spindles at earlier stages of spindle elongation, no microtubules with diameters markedly greater than 24 nm were found in the terminal (4- $\mu\text{m}$ -long) portions of spindles. Cross-sections close to the ends of spindles (within 0.5  $\mu\text{m}$  of terminal knobs) contained some microtubules with diameters  $<24 \text{ nm}$  (20–22 nm) (Fig. 10). These unusually small dimensions are perhaps related to the fact that many microtubules in these sections were being cut within 0.5  $\mu\text{m}$  of their tips. Here microtubule wall structure may have been atypical and/or have responded differently to fixation compared with other points along a microtubule's length.

Fixation in the presence of tannic acid was done to detect protofilaments. Because of the difficulties involved in obtaining good cross-sections of spindles shorter than  $\sim 60 \mu\text{m}$  (see

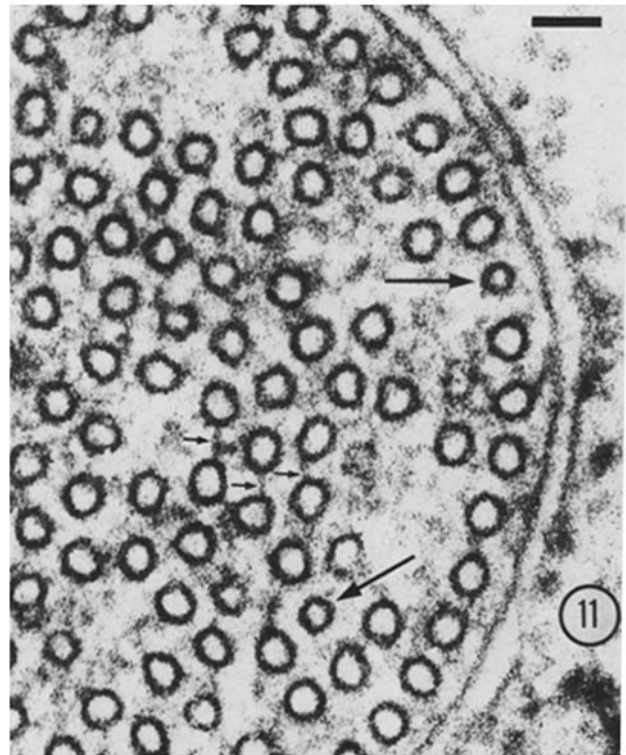
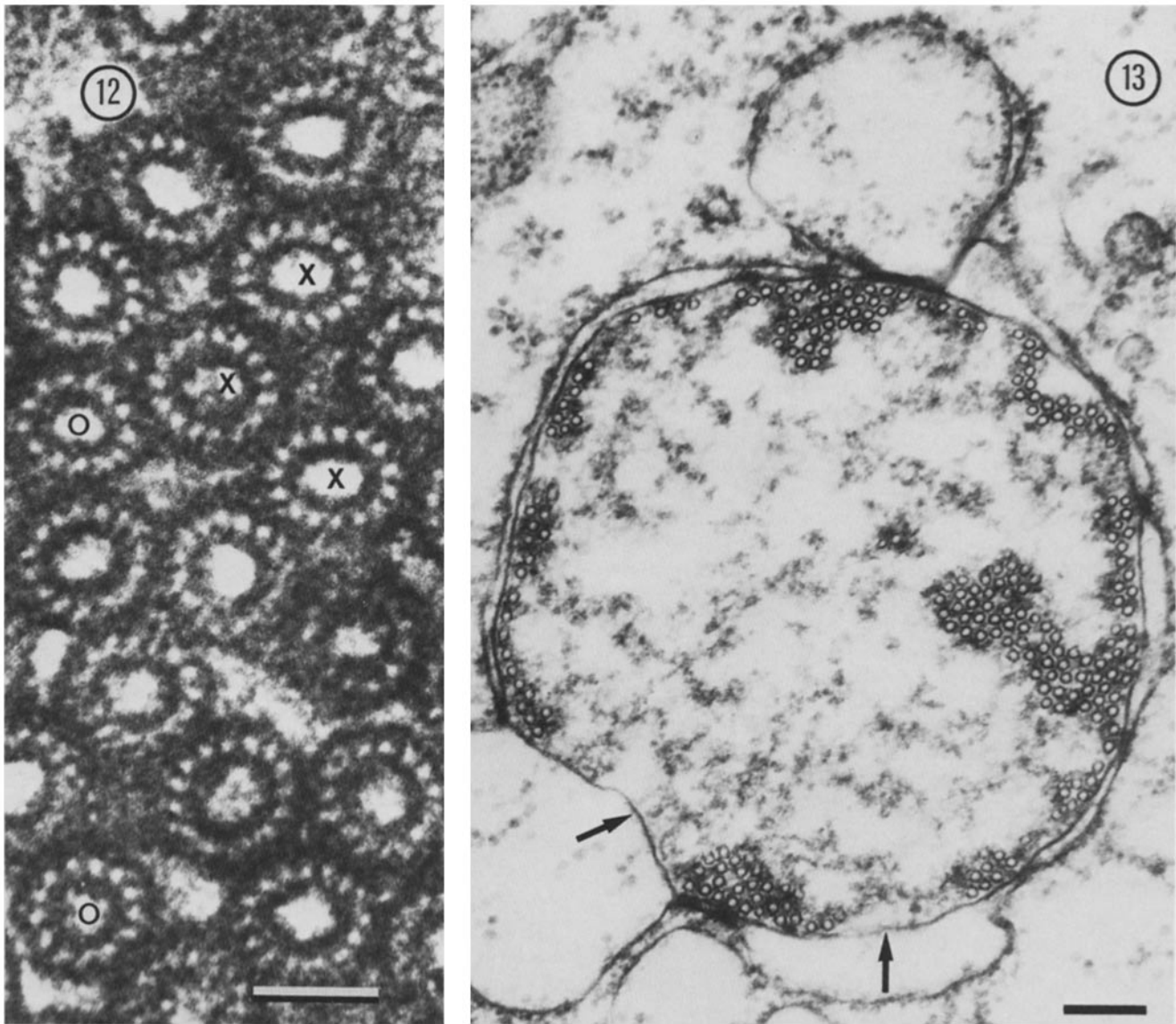


FIGURE 11 Cross-section through a portion of a 65- $\mu\text{m}$ -long spindle cut close to its midpoint. Although most of the microtubules have diameters of 27–32 nm, several microtubules with diameters of  $\sim 24 \text{ nm}$  are present (long arrows). Some microtubules are connected by intertubule links (short arrows), and some of the microtubules at the spindle periphery are joined to the nuclear envelope by dense bridges. Bar, 50 nm.  $\times 190,000$ .

Materials and Methods), and because the terminal portions of spindles at all stages were usually slightly curved out of alignment with the remainder of a spindle and the longitudinal axes of dividing cells, information was only obtained for the midportions of well-elongated spindles. Furthermore, unequivocal counts of the number of protofilaments/microtubule cross-section were only possible for  $<4\%$  of the microtubules included in each spindle cross-section. The remainder of the microtubules were not sufficiently well oriented to permit clear detection of all the protofilaments in their cross-sectional profiles (Fig. 12). Most of the microtubules in all portions of well-elongated spindles that were examined (i.e., all of the spindles except the 4- $\mu\text{m}$ -long terminal portions) were composed of more than 13 protofilaments. For microtubule profiles in which all protofilaments could be clearly distinguished 17% were composed of 16 protofilaments, 68% of 15 protofilaments, 2% of 14 protofilaments, and 13% of 13 protofilaments.

At least some of the microtubules in the midportions of well-elongated spindles were connected at various points along their lengths by components that resembled intertubule links (Fig. 11). Microtubules at the peripheries of well-elongated spindles were fairly regularly spaced, positioned close to the nuclear envelope, and sometimes joined to the envelope by dense bridges like the peripheral sheath microtubules of shorter spindles (Fig. 11). Evidence that such links and bridges may bind microtubules to each other and the envelope was obtained from examinations of organisms containing spindles with lengths of 36–65  $\mu\text{m}$  which had been exposed to a



FIGURES 12 and 13 (Fig. 12) Cross-section through a portion of a spindle fixed in the presence of tannic acid. The spindle had a length of  $62\ \mu\text{m}$  and was cut close to its midpoint. The spindle includes microtubules with 15 (X) and 13 (O) protofilaments. Bar,  $30\ \text{nm}$ .  $\times 628,000$ . (Fig. 13) Cross-section through a swollen spindle (compare Fig. 6) with a length of  $36\ \mu\text{m}$  cut near its midpoint in an organism that was exposed to a detergent-containing solution before fixation. A peripheral sheath-like layer of microtubules lines most of the inner surface of the nuclear envelope except in some regions where blebbing and swelling of the envelope is most pronounced (arrows). Bar,  $0.2\ \mu\text{m}$ .  $\times 62,500$ .

modified permeabilization medium (11) containing 0.1% Nonidet P-40 for 3 min before fixation. This treatment induced swelling of nuclear envelopes at several regions along the lengths of separation spindles. Where swelling had occurred, most microtubules remained closely grouped alongside each other as in untreated spindles. The peripheral sheath-like layer of microtubules remained associated with the nuclear envelope (Fig. 13). However, the layer was discontinuous. Gaps were mainly positioned where substantial blebbing of the outer membrane of the envelope had occurred (Fig. 13, arrows) and where, presumably, expansion of the inner membrane had also taken place.

#### *Final Stages of Spindle Elongation*

Although the number of microtubules/spindle cross-section (at the middles of spindles) only decreased from  $\sim 220$  to  $\sim 175$

as spindles elongated from  $\sim 35$  to  $\sim 70\ \mu\text{m}$  (Figs. 2, *b*, *c*, and *d*, 6, 8, and 9), this value decreased considerably as spindles lengthened beyond  $70\ \mu\text{m}$  (Fig. 14). Three spindles with lengths of  $76$ ,  $78$ , and  $84\ \mu\text{m}$  possessed 109, 85, and 125 microtubules, respectively, at their middles. Serial sectioning of the terminal portions of spindles showed that terminal knobs usually pinched off from separation spindles as spindles reached lengths of between  $78$  and  $87\ \mu\text{m}$ . Although separation spindles were functionally redundant after this stage, the number of microtubules/spindle cross-section near spindle midpoints continued to decrease. Whether spindles continued to elongate as this occurred was not ascertained. Eventually spindles pinched in half near their midpoints shortly ( $\sim 2$  min) before the completion of cell cleavage.

In nearly all of the organisms examined, at least one of each organism's dividing micronuclei was situated closely alongside the dorsally located macronucleus (36), which was

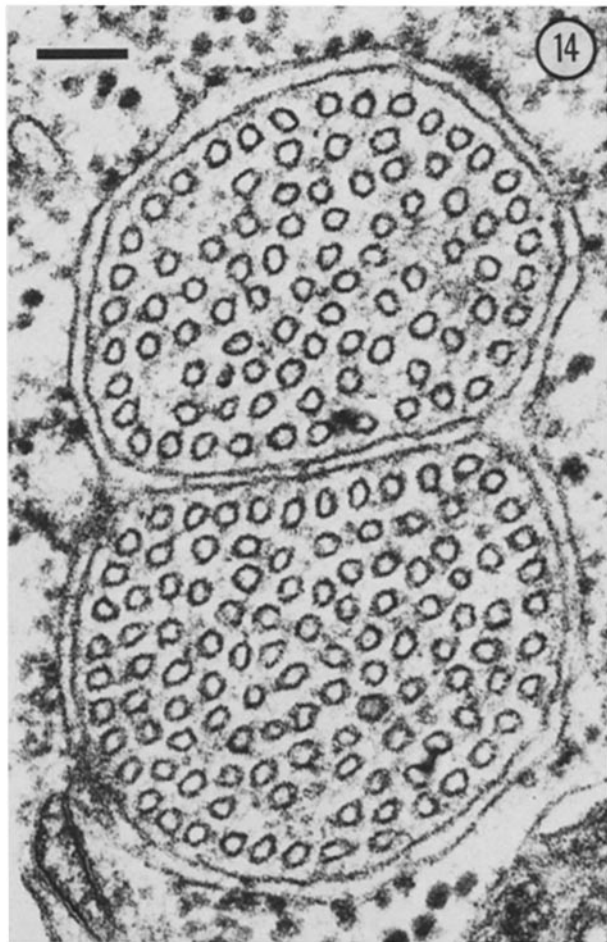


FIGURE 14 Cross-section close to the midpoints of two spindles with lengths of  $\sim 80 \mu\text{m}$ . The outer membranes of the nuclear envelopes of the two nuclei have fused together. Bar,  $0.1 \mu\text{m}$ .  $\times 120,000$ .

simultaneously elongating and dividing. In about one third of the organisms both micronuclei were located in this way and were closely juxtaposed. The outer membranes of the nuclear envelopes of micronuclei with lengths of  $65 \mu\text{m}$  or more were often fused together in regions where nuclei were positioned closely alongside each other (Fig. 14).

## DISCUSSION

There seem to be two distinct phases of spindle elongation: an early one during which large numbers of 24-nm-diam microtubules are present throughout the spindle (Fig. 15*a*), and one that follows after most of these microtubules have been eliminated from spindle midportions (Fig. 15, *b* and *c*).

### Microtubule Reorganization in the Elongating Spindle

As spindles elongate from  $\sim 20$  to  $35 \mu\text{m}$  there is a marked decrease in microtubule number/spindle cross-section in the midportions of spindles (from over 1,000 to  $\sim 200$ ). A very substantial decrease in spindle microtubule content (from 12.3 to 4.7  $\mu\text{m}$ ) also occurs during this period. Hence, the decrease in microtubule number/spindle cross-section must involve the disassembly of most of the microtubules that were situated in spindle midportions, rather than only being an

indication of microtubule sliding and a decrease in microtubule overlap at the middles of spindles. It is perhaps heretical to argue that most microtubules disassemble in a microtubule bundle that has recently started to elongate at a rate of  $8 \mu\text{m}/\text{min}$  and has still to lengthen for a further  $50 \mu\text{m}$  or more. However, it is the only conclusion that fits the facts. Substantial microtubule disassembly has also been found to occur during the marked elongation of spindles in the rust fungus *Puccinia malvacearum* (33), the yeast *Saccharomyces cerevisiae* (19), and in the separation spindles of *Nyctotherus ovalis* (8).

The assertion that a marked loss of spindle microtubules occurs is supported by the finding that most of the microtubules in spindles with lengths of up to  $21 \mu\text{m}$  have diameters of  $\sim 24 \text{ nm}$ , but that subsequently spindle midportions are populated almost entirely by microtubules with diameters of 27–32 nm (and more than 13 protofilaments) (Fig. 15). Correlations have been found in the midportions of well-elongated spindles (*a*) between the numbers of microtubules with 15–16 protofilaments and the numbers of microtubules with diameters of 27–32 nm, and (*b*) between the numbers of microtubules with 13 protofilaments and the numbers of microtubules with diameters of  $\sim 24 \text{ nm}$ . These correlations indicate that microtubules with diameters of 27–32 nm are composed of 15–16 protofilaments, and that most microtubules with diameters of  $\sim 24 \text{ nm}$  are composed of 13 protofilaments. If this is also the case at earlier stages of spindle elongation, then loss of microtubules is mainly achieved by disassembly of most of the 13 protofilament microtubules in spindle midportions, while most microtubules with more than 13 protofilaments remain intact. Disassembly of most microtubules with 13 protofilaments also takes place in the midportions of separation spindles in *Nyctotherus* at a relatively early stage of spindle elongation (8).

The case for retention of peripheral sheath microtubules in spindle middles and their reorganization for a major role in the subsequent stages of spindle elongation is as follows. Most of the 226 microtubules with diameters of 27–32 nm near the middle of the  $21\text{-}\mu\text{m}$ -long spindle were included in the peripheral sheath. A strikingly similar number of microtubules (219 and 228) remained at the middles of spindles, with lengths of 34 and  $36 \mu\text{m}$ , respectively, shortly after elimination of most 24-nm-diam microtubules from spindle midportions. Such spindles have a hollowed out appearance, and many of the microtubules still contribute to a distinct peripheral sheath (Fig. 15*b*). Subsequently, most microtubules are not closely associated with the nuclear envelope. Peripheral sheath microtubules apparently regroup so that they run closely alongside each other to form the compact bundle present during the later stages of spindle elongation (Fig. 15*c*).

### Design of the Early Spindle

Disassembly of microtubules in spindles with lengths of  $\sim 25 \mu\text{m}$  is selective. It mainly, perhaps entirely, involves breakdown of microtubules with diameters of  $\sim 24 \text{ nm}$ , but in addition, there is a spatial difference in the extent to which microtubules are eliminated from a spindle. The reduction in the number of 24-nm microtubules/spindle cross-section is much less marked in the terminal portions of spindles than it is in the middles of spindles (Fig. 15, *a* and *b*). This is also the case in the separation spindles of *Nyctotherus* (8). This pattern of microtubule breakdown may be an indication that



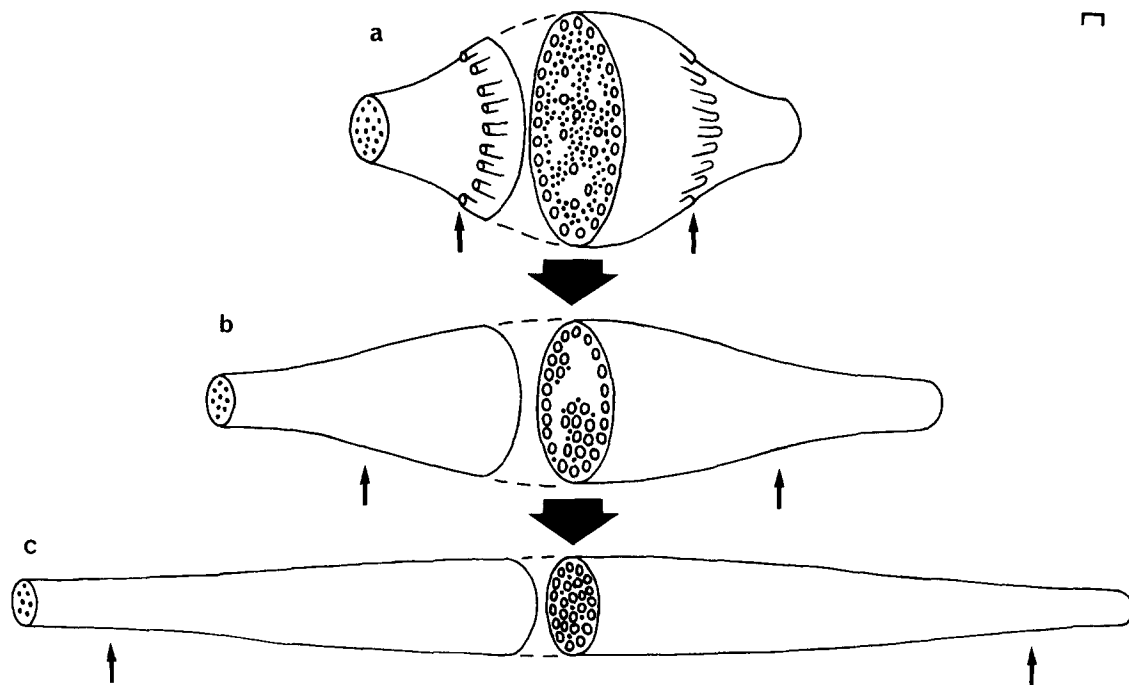


FIGURE 15 Schematic diagram showing the main changes in microtubule deployment as separation spindles elongate. Each spindle is shown with a sector removed to show microtubule arrangement at its midpoint. Small open circles represent cross-sectional profiles of microtubules with diameters of 27–32 nm (and more than 13 protofilaments in c); black dots represent microtubules with diameters of ~24 nm (and 13 protofilaments at the mid-point c). Spindles have been drawn to scale but for clarity the vertical axis is represented on a larger scale than the horizontal axis (scale bars, 1  $\mu\text{m}$ ) so that spindle diameters are shown disproportionately large ( $\times 5$ ) with respect to spindle lengths. In addition, microtubules are illustrated with diameters that are disproportionately large with respect to spindle diameters. The relative numbers of microtubules/spindle cross-section are accurately portrayed so far as different spindle regions, different stages in spindle elongation, and different types of microtubules are concerned (at 17% of the numbers that actually occur). Microtubules with diameters greater than 24 nm were not found in the terminal portions of spindles beyond positions indicated by the small arrows. (a) 21- $\mu\text{m}$ -long spindle showing the position of its peripheral sheath; (b) 34- $\mu\text{m}$ -long spindle; (c) 53- $\mu\text{m}$ -long spindle.

there are two main populations of 24-nm microtubules in the early spindles. If each population is mainly situated on either side of the spindle midpoint and disassembly takes place from the centrally directed ends of such microtubules, then spindle middles are likely to become more extensively depleted of microtubule portions than are spindle extremities. This hypothesis implies that conditions promoting release of tubulin from microtubule ends cease before the longest microtubules have been completely eliminated.

The possibility that there are two main populations of 24-nm microtubules of opposite polarity that are mainly distributed on either side of the midpoints of early spindles is pertinent to the initial mode of spindle elongation. The microtubule-free gaps at the middles of spindles (Fig. 15 a) may be an indication that microtubules with opposite polarities slide out from spindle midportions in opposite directions as a spindle starts to elongate. Such a mechanism seems to operate during the elongation of the central spindles of certain diatoms (26). Two sets of antiparallel microtubules that slide apart in this manner can, at most, only double the length of a spindle (unless microtubule elongation occurs to compensate for reduction in microtubule overlap before the two sets slide off the ends of each other) (31). Ciliates may have originally used this type of mechanism in their separation spindles and have subsequently evolved further sophistications to achieve the spindle elongations of up to an order of magnitude and more that are found in some contemporary

forms. For example, the peripheral sheath that is anchored to the nuclear envelope in the middle of the spindle may be one such sophistication. The sheath might have initially evolved to maintain the structural integrity of the spindle midportion (Fig. 15 a), when the other microtubules slide out from its interior, by postponing the stage at which loss of microtubule overlap occurs. The disassembly of 24-nm microtubules and regrouping of sheath microtubules considered above (Fig. 15, b and c) may represent a second mode of spindle elongation that has only evolved in the more advanced ciliates. Spindles only elongate by ~70%, from 12  $\mu\text{m}$  at metaphase to final lengths of ~20  $\mu\text{m}$ , during micronuclear mitosis in *Loxodes magnus* (28). This organism has been assigned to the order Karyorelictida because of the apparently primitive nature of the organization of its macronuclei (29).

#### Main Phase of Spindle Elongation

There is a considerable increase in spindle microtubule content (from 4.7 to 8 mm) as spindles lengthen from 34 to 67  $\mu\text{m}$ . Hence, substantial microtubule polymerization is involved and, furthermore, there is no marked change in microtubule number/spindle cross-section at the middles of spindles during this main phase of spindle elongation. Microtubules with diameters of 27–32 nm and 15–16 protofilaments predominate along most of the lengths of spindles (for more than 60  $\mu\text{m}$  along spindles with lengths of ~70  $\mu\text{m}$ ). There are also indications that these microtubules may span

spindle mid-portions. Hence, most of spindle lengthening could be accounted for by further elongation of the microtubules with diameters of 27–32 nm (mainly peripheral sheath microtubules) that are already present before the microtubule disassembly phase, without initiation of the assembly of any additional microtubules.

The possibility that a certain amount of microtubule sliding occurs and generates essential forces has not been eliminated. For example, there is a decrease of ~20% in the numbers of microtubules/spindle cross-section at the middles of spindles as spindles lengthen from ~35  $\mu\text{m}$  to ~70  $\mu\text{m}$ . Furthermore, microtubule elongation that is occurring during this period may compensate to some extent for reduction in microtubule overlap that would otherwise occur if intertubule sliding is taking place.

Why do about 800 microtubule portions disassemble before a period of microtubule polymerization and the main phase of spindle elongation? It may be to effect more economical use of microtubule proteins. For example, far less tubulin is needed for spindle elongation than would otherwise be the case (especially if tubulin released during the disassembly of 24-nm microtubules is recycled as polymerization of microtubules with 14–16 protofilaments continues).

### Final Stages of Spindle Elongation

Intertubule sliding may also occur during the final stages of spindle elongation and account for the decreases in microtubule number/spindle cross-section that take place as spindles lengthen from ~70 to 85  $\mu\text{m}$ . Such sliding might provide a basis for the final central fission of spindles.

Why do nuclear envelopes around spindle middles tend to fuse together during the final stages of spindle elongation? This tendency might have evolved as an additional safeguard to prolong the linear integrity of dividing nuclei in cases where central fission of one of an organism's two micronuclear separation spindles occurs at an unusually early stage with respect to cell cleavage. Such a strategy apparently operates in a more elaborate form in the ciliate *Nassula* where the envelopes of all three dividing micronuclei fuse with each other and that of the elongating macronucleus (34).

### Spindle Construction and Elongation— The Major Issues

Variation in protofilament number provides a basis for microtubule differentiation in the separation spindle. For example, microtubules with more than 13 protofilaments elongate during a period when microtubules with 13 protofilaments are disassembling. Furthermore, microtubules with more than 13 protofilaments do not appear to be distributed at random throughout the spindle. Comparisons of microtubule diameters indicate that most of these microtubules are concentrated in a sheath-like array that is associated with the nuclear envelope during early stages of spindle elongation and that they do not occur in the terminal portions of spindles. Examinations of early mitotic stages are needed to ascertain whether assembly of microtubules with more than 13 protofilaments is nucleated at sites that are distinct from those where microtubules with 13 protofilaments are initiated.

The functional significance of exploiting variation in protofilament number as a mode for microtubule differentiation is not immediately obvious because the roles of the different

classes of microtubules are not fully established. The changes in the numbers and positioning of microtubules in spindle cross-sections reported above are difficult to interpret in functional terms since microtubules are assembling and depolymerizing simultaneously, and are probably sliding over each other as well. Detailed tracking of individual microtubules to ascertain the spatiotemporal pattern of changes in microtubule lengths and overlap as spindles elongate will be rewarding in this context.

The spatial relationship between the peripheral sheath and the microtubules that lie inside it (Fig. 15) is especially compatible with the suggestion that a spindle may function like a telescoping sleeve during anaphase B to guide sister chromatids to opposite ends of the cell and/or govern separation rate (20). The important question (see reference 18) of whether the separation spindle actively pushes chromatids apart (2–4), or alternatively, provides a framework that is extended by forces that are generated outside the spindle (20) and are applied to the exterior of the nucleus (1), remains to be resolved. The demonstration of a marked switch in spindle microtubule organization as anaphase progresses in *Paramecium* is particularly important in this context. It is another indication (27, 33) that anaphase B is promoted by more than one distinct force-generating mechanism in certain organisms.

We thank Ian Roberts (Scottish Horticultural Research Institute, Invergowrie, Angus, UK) for instruction in the use of crystalline catalase for microscope calibration.

Received for publication 23 April 1985, and in revised form 1 August 1985.

### REFERENCES

- Aist, J. R., and M. W. Berns. 1981. Mechanics of chromosome separation during mitosis in *Fusarium* (Fungi imperfecti): new evidence from ultrastructural and laser microbeam experiments. *J. Cell Biol.* 91:446–458.
- Bajer, A. S., C. Cypher, J. Mole-Bajer, and H. M. Howard. 1982. Taxol-induced anaphase reversal: evidence that elongating microtubules can exert a pushing force in living cells. *Proc. Natl. Acad. Sci. USA.* 79:6569–6573.
- Cande, W. Z. 1982. Nucleotide requirements for anaphase chromosome movements in permeabilized mitotic cells: anaphase B but not anaphase A requires ATP. *Cell.* 28:15–22.
- Cande, W. Z., and K. L. McDonald. 1985. *In vitro* reactivation of anaphase spindle elongation using isolated diatom spindles. *Nature (Lond.)* 316:168–170.
- Cohen, J., J. Beisson, and J. B. Tucker. 1980. Abnormal microtubule deployment during defective macronuclear division in a *Paramecium* mutant. *J. Cell Sci.* 44:153–167.
- Davidson, L., and J. R. LaFountain. 1975. Mitosis and early meiosis in *Tetrahymena pyriformis* and the evolution of mitosis in the phylum Ciliophora. *Biosystems.* 7:326–336.
- Eichenlaub-Ritter, U. 1982. Micronuclear mitosis in the ciliate *Nyctotherus ovalis* Leidy: an unusual chromosome arrangement and kinetochore structure and its implications for spindle structure and function. In *Microtubules in Micro-Organisms*. P. Cappuccinelli and N. R. Morris, editors. Marcel Dekker, Inc., New York. 351–375.
- Eichenlaub-Ritter, U. 1985. Spatiotemporal control of functional specification and distribution of spindle microtubules with 13, 14 and 15 protofilaments during mitosis in the ciliate *Nyctotherus*. *J. Cell. Sci.* In press.
- Eichenlaub-Ritter, U., and A. Ruthmann. 1982. Holokinetic composite chromosomes with "diffuse" kinetochores in the micronuclear mitosis of a heterotrichous ciliate. *Chromosoma.* 84:701–716.
- Eichenlaub-Ritter, U., and A. Ruthmann. 1982. Evidence for three "classes" of microtubules in the inter-polar space of the mitotic micronucleus of a ciliate and the participation of the nuclear envelope in conferring stability to microtubules. *Chromosoma.* 85:687–706.
- Eichenlaub-Ritter, U., and J. B. Tucker. 1984. Microtubules with more than 13 protofilaments in the dividing nuclei of ciliates. *Nature (Lond.)* 307:60–62.
- Grell, K. G., and A. Meister. 1984. Contribution to the ultrastructure of conjugation of *Ephelota gemmipara* R. Hertwig (Suctorina). *Protistologica.* 20:65–86.
- Inoué, S., and H. Ritter. 1975. Dynamics of mitotic spindle organization and function. In *Molecules and Cell Movement*. S. Inoué and R. E. Stephens, editors. Raven Press, New York. 3–30.
- Jenkins, R. A. 1981. The dynamics of micronuclear mitosis in the living ciliate *Spirostomum teres* as revealed by polarization microscopy. *J. Protozool.* 28:393–399.
- Jurand, A. 1976. Some ultrastructural features of micronuclei during conjugation and autogamy in *Paramecium aurelia*. *J. Gen. Microbiol.* 94:193–203.
- Jurand, A., and G. G. Selman. 1969. The Anatomy of *Paramecium aurelia*. Macmillan and Co. Ltd., London. 1–218.
- Jurand, A., and G. G. Selman. 1970. Ultrastructure of the nuclei and intranuclear microtubules of *Paramecium aurelia*. *J. Gen. Microbiol.* 60:357–364.

18. King, S. M. 1983. Multiple mechanisms of mitosis? *Nature (Lond.)* 301:660.
19. King, S. M., J. S. Hyams, and A. Luba. 1982. Absence of microtubule sliding and an analysis of spindle formation and elongation in isolated mitotic spindles from the yeast *Saccharomyces cerevisiae*. *J. Cell. Biol.* 94:341-349.
20. Kronebusch, P. J., and G. G. Borisy. 1982. Mechanics of anaphase B movement. In *Biological Functions of Microtubules and Related Structures*. H. Sakai, H. Mohri, and G. G. Borisy, editors. Academic Press, Inc., New York. 233-245.
21. LaFountain, J. R., and L. A. Davidson. 1979. An analysis of spindle ultrastructure during prometaphase and metaphase of micronuclear division in *Tetrahymena*. *Chromosoma* 75:292-308.
22. LaFountain, J. R., and L. A. Davidson. 1980. An analysis of spindle ultrastructure during anaphase of micronuclear division in *Tetrahymena*. *Cell Motil.* 1:41-61.
23. Lewis, L. M. 1975. The evolutionary significance of ultrastructural variations in the micronuclear spindle apparatus in the genus *Paramecium*. *Biosystems* 7:380-385.
24. Lewis, L. M., W. R. Witkus, and G. M. Vernon. 1976. Role of microtubules and microfilaments in the micronucleus of *Paramecium bursaria* during mitosis. *Protoplasma* 89:203-219.
25. McIntosh, J. R. 1979. Cell Division. In *Microtubules*. K. Roberts and J. Hyams, editors. Academic Press, London. 381-441.
26. Pickett-Heaps, J. D., and D. H. Tippit. 1978. The diatom spindle in perspective. *Cell* 14:455-467.
27. Pickett-Heaps, J. D., D. H. Tippit, and K. R. Porter. 1982. Rethinking mitosis. *Cell* 29:729-744.
28. Raikov, I. 1973. Mitose intranucléaire du micronoyau de *Loxodes magnus*, cilié holotriche. Etude ultrastructurale. *Compte Rendus Acad. Sci. (Paris)* 276(D):2385-2388.
29. Raikov, I. B. 1982. *The Protozoan Nucleus. Morphology and Evolution*. Springer-Verlag, Vienna. 1-474.
30. Sonneborn, T. M. 1975. The *Paramecium aurelia* complex of fourteen sibling species. *Trans. Am. Microsc. Soc.* 94:155-178.
31. Soranno, T., and J. D. Pickett-Heaps. 1982. Directionally controlled spindle disassembly after mitosis in the diatom *Pinnularia*. *Eur. J. Cell Biol.* 26:234-243.
32. Stevenson, I., and F. P. Lloyd. 1971. Ultrastructure of nuclear division in *Paramecium aurelia*. I. Mitosis in the micronucleus. *Aust. J. Biol. Sci.* 24:963-975.
33. Tippit, D. H., C. T. Fields, K. L. O'Donnell, J. D. Pickett-Heaps, and D. J. McLaughlin. 1984. The organization of microtubules during anaphase and telophase spindle elongation in the rust fungus *Puccinia*. *Eur. J. Cell Biol.* 34:34-44.
34. Tucker, J. B. 1967. Changes in nuclear structure during binary fission in the ciliate *Nassula*. *J. Cell Sci.* 2:481-498.
35. Tucker, J. B. 1979. Spatial organization of microtubules. In *Microtubules*. K. Roberts and J. Hyams, editors. Academic Press, London. 315-357.
36. Tucker, J. B., J. Beisson, D. L. J. Roche, and J. Cohen. 1980. Microtubules and control of macronuclear 'amitosis' in *Paramecium*. *J. Cell. Sci.* 44:135-151.
37. Wolfe, J., B. Hunter, and W. S. Adair. 1976. A cytological study of micronuclear elongation during conjugation in *Tetrahymena*. *Chromosoma* 55:289-308.
38. Wrigley, N. G. 1968. The lattice spacing of crystalline catalase as an internal standard of length in electron microscopy. *J. Ultrastruct. Res.* 24:454-464.